Modeling Uncertainty of Renewable Energy in Microgrid Dispatch Using Scenario-Based Risk-Aware Optimization

DAVID O. BRICEÑO, DIANA S. LÓPEZ, SERGIO R. RIVERA
Departamento de Ingeniería Eléctrica y Electrónica
Universidad Nacional de Colombia
Ave Cra 30 #45-3 Bogotá D.C.
COLOMBIA

Abstract: This paper presents a probabilistic and risk-aware framework for microgrid dispatch under renewable generation. In this way, solar irradiance is modeled using a log-normal distribution, on other hand, wind speed follows a Rayleigh distribution. We used a combined multi-regime wind turbine power curve for the eolic part. A scenario-based Monte Carlo approach got multiple realizations of renewable output per hour, enabling the explicit evaluation of intermittence or stochastic variability. In order to quantify operational risk, we formulate Uncertainty Cost Functions that integrates: (i) the expected operational cost, (ii) the Conditional Value-at-Risk (CVaR), and (iii) the variability of the battery State of Charge (SOC). The proposed approach is validated in a microgrid with solar, wind, battery storage, and flexible loads. Results demonstrate that the risk-aware dispatch significantly reduces tail-risk exposure, mitigates SOC fluctuations, and enhances operational resilience when compared to a conventional risk-neutral strategy.

Key-Words: Microgrids; Renewable Uncertainty; Scenario-Based Optimization; CVaR; Risk-Aware Dispatch; Demand Response; Battery Storage; Stochastic Modeling

Received: May 23, 2025. Revised: September 11, 2025. Accepted: December 14, 2025. Published: May 13, 2026.

1 Introduction

The increasing penetration of renewable energy resources in modern microgrids has introduced significant operational challenges, primarily due to the stochastic nature of photovoltaic (PV) and wind generation. Unlike conventional dispatchable resources, renewable output is subject to rapid and unpredictable fluctuations caused by environmental variability. Solar irradiance exhibits strong diurnal patterns affected by cloud cover and atmospheric conditions, while wind speed follows nonlinear, site-dependent distributions. As a result, energy balancing, storage coordination, and cost optimization become more complex when uncertainty is not explicitly considered in the dispatch strategy, [1], [2].

Traditional deterministic microgrid controllers rely on expected values or forecasted power profiles, which ignore the inherent uncertainty and may lead to risk-prone decisions, [3] . These approaches can underestimate the frequency and impact of adverse events such as sudden drops in renewable output, simultaneous load peaks, or insufficient stored energy. To mitigate such risks, probabilistic and scenario-based frameworks have emerged as effective tools for characterizing renewable variability, [1]. Log-normal models capture the positive skewness of solar irradiance, while Rayleigh distributions are widely used to describe wind speed behavior. However, incorporating probabilistic modeling alone is insufficient without a mechanism capable of quantifying the operational risk associated with extreme scenarios, [4], [5].

Coherent risk metrics provide a mathematically robust means of capturing tail events beyond the coverage of conventional expectation-based metrics, [3]. Among them, the Conditional Value-at-Risk (CVaR) is particularly relevant for microgrid dispatch, as it measures the expected cost in the worst-case α-tail of the distribution. CVaR has been successfully adopted in optimization problems requiring resilience against low-probability, high-impact events, making it suitable for decision-making under renewable uncertainty, [2].

In parallel, Demand Response (DR) has become a key flexibility mechanism in microgrids, allowing users to strategically adapt their consumption according to system conditions, [4], [5]. In this context, users may choose between cooperative actions, which reduce their demand to alleviate system stress, or competitive actions that preserve consumption at the expense of higher operational cost. The selection of these strategies strongly depends on renewable availability, storage conditions, and perceived risk, [5].

In this work, we propose a comprehensive scenario-based, risk-aware dispatch framework that integrates probabilistic modeling of renewable generation, energy storage dynamics, and user-driven DR strategies, [3]. The core of the proposed method is an Uncertainty Cost Function (UCF) that combines the expected operational cost, the CVaR of scenario-based renewable uncertainty, and the variability of the battery State of Charge (SOC). At each hour, the microgrid evaluates multiple renewable scenarios and selects the DR action that minimizes the UCF, resulting in a robust strategy that accounts for both typical and extreme operating conditions, [3].

In this way, the art state of integration of variable renewable energy sources in modern microgrids introduces operational complexities due to their non-deterministic behavior. This work outlines the modeling approach, risk quantification methodology, and decision-making strategy employed to address these challenges, [6].

1.1 Probabilistic Characterization of Renewable Generation

The power output from photovoltaic (PV) systems and wind turbines is modeled using probability distributions that capture their inherent variability:

$$f_{\text{solar}}(x) = \frac{1}{x\sigma\sqrt{2\pi}} \exp\left(-\frac{(\ln x - \mu)^2}{2\sigma^2}\right) \quad (1)$$

$$f_{\text{wind}}(v) = \frac{v}{c^2} \exp\left(-\frac{1}{2}\left(\frac{v}{c}\right)^2\right) \quad (2)$$

where equation (1) represents the log-normal distribution for solar irradiance and equation (2) represents the Rayleigh distribution for wind speed, [4].

1.2 Risk-Aware Optimization Framework

The operational decision-making process incorporates a multi-objective function that balances expected cost with risk mitigation (3):

$$\text{UCF} = \mathbb{E}[C] + \lambda_1 \cdot \text{CVaR}\alpha + \lambda_2 \cdot \sigma\text{SOC} \quad (3)$$

where:

- $\mathbb{E}[C]$: Expected operational cost
- CVaRα: Conditional Value-at-Risk at confidence level α
- σSOC: Standard deviation of State of Charge
- λ_1, λ_2: Risk aversion parameters

1.3 Performance Metrics and Evaluation

The proposed framework is evaluated using the following comparative metrics, [6], equations (4), (5) and (6):

$$\text{Risk Reduction} = \frac{\text{CVaRdet} - \text{CVaRproposed}}{\text{CVaR}_{\text{det}}} \quad (4)$$

$$\text{SOC Stability} = 1 - \frac{\sigma_{\text{SOC}}}{\text{SOCmax} - \text{SOCmin}} \quad (5)$$

$$\text{Cost Robustness} = \frac{C_{\text{worst-case}} - C_{\text{expected}}}{C_{\text{expected}}} \quad (6)$$

1.4 Methodological Contributions

The main contributions of this paper can be summarized as follows:

- The development of an uncertainty-aware microgrid dispatch framework that integrates stochastic renewable generation, battery dynamics, and strategic demand response decisions.
- The formulation of a unified Uncertainty Cost Function that combines expected operating cost, Conditional Value-at-Risk, and battery state-of-charge variability.
- A scenario-based evaluation approach using probabilistic renewable models, aligned with commonly accepted representations of solar irradiance and wind speed.
- A game-theoretic interpretation of demand response actions, allowing flexible users to adopt cooperative or competitive strategies under uncertainty.
- A numerical assessment demonstrating that the proposed framework reduces tail-risk and improves storage stability when compared to a deterministic baseline.

The remainder of this paper is structured as follows. Section 2 presents the probabilistic modeling of solar and wind resources. Section 3 describes the microgrid architecture and storage dynamics. Section 4 introduces the DR model and user strategies. Section 5 formulates the risk-aware optimization problem and UCF. Section 6 details the proposed algorithm. Section 7 presents the numerical results, and Section 8 concludes the paper.

2 Probabilistic Modeling of Renewable Resources

Accurate representation of renewable energy variability is essential for risk-aware microgrid dispatch. In this work, we employ probabilistic distributions that capture the stochastic characteristics of solar irradiance and wind speed without relying on deterministic forecasts, [5], [6]. These models serve as the basis for the generation of multiple Monte Carlo scenarios used in the risk evaluation process, [1], [5].

2.1 Solar Irradiance Modeling

Solar irradiance exhibits strong diurnal patterns combined with high short-term variability caused by cloud cover and atmospheric conditions. To capture this behavior, we model irradiance G_t using a log-normal probability distribution, which effectively represents the positive skewness observed in empirical data. The probability density function (PDF) is given by equation (7), [4], [7], [8]:

$$f_G(g) = \frac{1}{g\sigma_G\sqrt{2\pi}} \exp\left(-\frac{(\ln g - \mu_G)^2}{2\sigma_G^2}\right), \quad (7)$$

where μ_G and σ_G denote the log-mean and log-standard deviation of the irradiance. These parameters can be computed from the empirical mean $\bar{G}$ and variance σ_G^2 using the standard relations (equation (8)) [9], [10]:

$$\mu_G = \ln\left(\frac{\bar{G}^2}{\sqrt{\bar{G}^2 + \sigma_G^2}}\right), \qquad \sigma_G^2 = \ln\left(1 + \frac{\sigma_G^2}{\bar{G}^2}\right). \quad (8)$$

The solar PV generation at time t is modeled as (equation (9)), [11]:

$$P_{PV}(t) = \eta_{PV} A_{PV} G_t, \quad (9)$$

where η_{PV} is the conversion efficiency and A_{PV} is the effective panel area. In our implementation, the irradiance is further modulated by a deterministic clear-sky envelope centered around midday, ensuring that nighttime generation remains zero, [5], [12].

As shown in Fig. 1, the resulting irradiance distribution presents a pronounced right-tail, which is consistent with empirical measurements of solar radiation under variable atmospheric conditions.

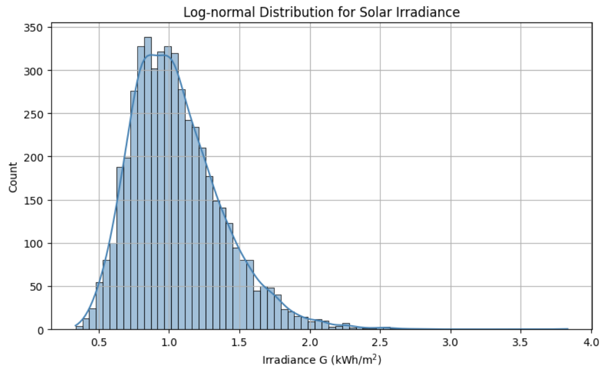

Fig. 1: Log-normal distribution used for modeling solar irradiance. Source: created by the authors.

2.2 Wind Speed Modeling

Wind speed is widely modeled using the Rayleigh distribution, which is a special case of the Weibull family and accurately captures wind behavior in locations with moderate turbulence. The PDF of the Rayleigh distribution is expressed as equation (10), [1], [13], [14]:

$$f_V(v) = \frac{v}{\sigma_V^2} \exp\left(-\frac{v^2}{2\sigma_V^2}\right), \quad (10)$$

where σ_V is the scale parameter characterizing the wind regime. In this way, we have:

Theorem 1 (Convergence of Wind Power Sampling)**.** *Under the Rayleigh model with scale parameter σ_V, the average wind power converges almost surely (equation 11):*

$$\lim_{M\to\infty} \frac{1}{M} \sum_{m=1}^{M} P_W^{(m)} = \int_0^\infty P_w(v) f_V(v)\, dv, \quad (11)$$

where $P_w(v)$ is defined in Eq. 12.

The Rayleigh distribution captures the typical unimodal and right-skewed behavior of wind speed, as illustrated in Figure 2.

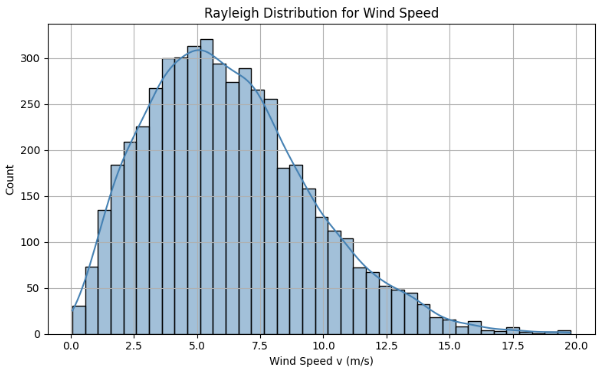

Fig. 2: Rayleigh distribution used for modeling wind speed. Source: created by the authors.

2.3 Wind Turbine Power Curve

The conversion from wind speed to electrical power is nonlinear and governed by the turbine's power curve. We adopt a multi-segment model defined as [4], [6]:

$$P_w(v) = \begin{cases} 0, & v < v_{ci} \\ P_{rated}\left(\frac{v^3 - v_{ci}^3}{v_r^3 - v_{ci}^3}\right), & \text{if } v_{ci} \leq v < v_r, \\ P_{rated}, & v_r \leq v < v_{co}, \\ 0, & v \geq v_{co}. \end{cases} \tag{12}$$

where v_{ci}, v_r, and v_{co} denote the cut-in, rated, and cut-out speeds, respectively. This representation captures the cubic rise in power between the cut-in and rated speeds, the plateau at rated power, and the shutdown behavior under excessive wind conditions, [8], [12].

The corresponding power conversion characteristics are shown in Figure 3, where the Cut-in, Rated, and Cut-out speeds are clearly reflected, [6], [13].

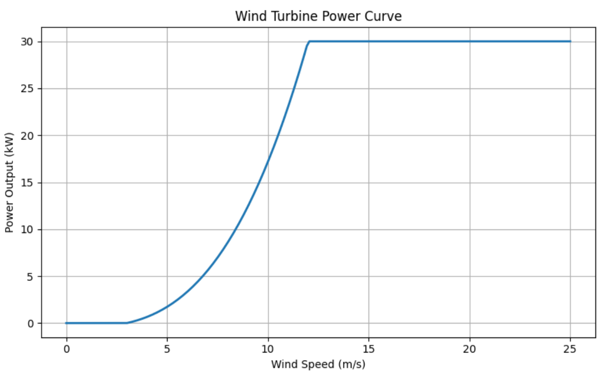

Fig. 3: Wind turbine power curve used in the wind generation model. Source: created by the authors.

The combination of equations (7) and (12) enables the generation of multiple renewable scenarios per hour. These scenarios are later used in the computation of expected cost and CVaR, forming the foundation of the risk-aware optimization framework described in Section 5.

3 Microgrid Model and Storage Dynamics

The microgrid considered in this work consists of photovoltaic (PV) generation, wind power generation, a battery energy storage system (BESS), and two flexible consumers capable of participating in demand response (DR), [4]. The microgrid operates in islanded mode and must maintain energy balance internally at each hourly time step. Renewable generation and user behavior are subject to uncertainty, making storage and DR essential components for achieving operational reliability, we used the structure proposed in [14], [15], [16], and it was included the uncertainty quantification matter, [17].

3.1 System Architecture

The microgrid includes solar PV panels modeled using the probabilistic irradiance distribution described in Section 2, and a wind turbine characterized by the Rayleigh wind speed distribution and the power curve in (12) and (13). The total renewable generation at time t is given by

$$P_{\text{RES}}(t) = P_{PV}(t) + P_W(t). \tag{13}$$

The load side of the microgrid is composed of two flexible users whose nominal demand profiles are denoted by $L_1(t)$ and $L_2(t)$. These users participate in DR by selecting cooperative or competitive actions, resulting in modified demand profiles $L_1^{\text{DR}}(t)$ and $L_2^{\text{DR}}(t)$.

The total demand at time t after DR adjustments is (14):

$$L_{\text{tot}}(t) = L_1^{\text{DR}}(t) + L_2^{\text{DR}}(t). \tag{14}$$

In the proposed model, two flexible users are introduced to capture the essential strategic interactions within a shared microgrid. Each user represents a group of adaptable loads that can lower their consumption in response to changing system conditions. While the model focuses on only two users, this simplification is enough to highlight how cooperation or competition can influence overall risk and the behavior of storage systems. Expanding the framework to include more users is a straightforward extension of the current approach and is reserved for future work.

3.2 Battery Energy Storage System

The BESS plays a key role in mitigating renewable variability and maintaining energy balance. We denote the state of charge (SOC) of the battery at time t as $SOC(t)$, with physical bounds (15), [5]:

$$0 \leq SOC(t) \leq SOC_{\max}. \tag{15}$$

Charging and discharging are subject to efficiency factors η_{ch} and η_{dis}, respectively. The battery power $P_{\mathrm{bat}}(t)$ is defined as positive during discharging and negative during charging.

3.3 SOC Update Equation

The SOC evolves according to the following equation (16):

$$SOC(t+1) = \begin{cases} SOC(t) + \eta_{\mathrm{ch}}\, P_{\mathrm{ch}}(t), & P_{\mathrm{bat}}(t) < 0, \\ SOC(t) - \dfrac{P_{\mathrm{dis}}(t)}{\eta_{\mathrm{dis}}}, & P_{\mathrm{bat}}(t) > 0, \end{cases} \tag{16}$$

where $P_{\mathrm{ch}}(t) = -P_{\mathrm{bat}}(t)$ represents charging power and $P_{\mathrm{dis}}(t) = P_{\mathrm{bat}}(t)$ represents discharging power.

Charging and discharging rates are limited by (17):

$$0 \leq P_{\mathrm{ch}}(t) \leq P_{\mathrm{ch}}^{\max}, \qquad 0 \leq P_{\mathrm{dis}}(t) \leq P_{\mathrm{dis}}^{\max}. \tag{17}$$

3.4 Energy Balance Constraint

At each hour, the microgrid must satisfy the balance between renewable generation, battery operation, and flexible demand (18):

$$P_{\mathrm{RES}}(t) + P_{\mathrm{bat}}(t) = L_{\mathrm{tot}}(t). \tag{18}$$

Given the uncertainty in $P_{\mathrm{RES}}(t)$, the battery and DR actions play a critical role in ensuring that the microgrid remains feasible and avoids energy shortages or excessive curtailment.

3.5 Role of Storage in Risk Mitigation

Variability in the SOC is directly linked to the ability of the microgrid to withstand periods of low renewable availability. High volatility in the SOC implies a higher probability of energy shortfalls, motivating the inclusion of an SOC variability term in the Uncertainty Cost Function introduced in Section 5. By penalizing deviations in SOC, the model promotes operational stability and ensures a more robust response to renewable fluctuations.

4 Demand Response Model and Strategic User Behavior

Demand Response (DR) is a key flexibility mechanism that enables consumers to adjust their demand in response to system conditions. In the context of a microgrid with uncertain renewable generation, DR plays an essential role in mitigating variability and ensuring operational reliability. In this work, two flexible users participate in DR by selecting between cooperative or competitive actions at every time step. These actions modify their baseline demand and influence the overall energy balance of the microgrid, [2].

4.1 Baseline Load Profiles

Let $L_1(t)$ and $L_2(t)$ denote the baseline hourly demand of User 1 and User 2, respectively. These profiles represent the consumption that would occur in the absence of DR. The total baseline demand at time t is therefore (19):

$$L_{\mathrm{base}}(t) = L_1(t) + L_2(t). \tag{19}$$

4.2 Cooperative and Competitive DR Actions

Each user may choose to either cooperate with the system or compete according to individual preferences and system conditions. These actions lead to adjusted demand levels that reduce or maintain consumption relative to the baseline. The DR-adjusted demand for user i at time t is modeled as (20):

$$L_i^{\mathrm{DR}}(t) = \begin{cases} (1-\gamma_c)L_i(t), & \text{cooperative action}, \\ (1-\gamma_k)L_i(t), & \text{competitive action}, \end{cases} \tag{20}$$

where γ_c and γ_k represent the cooperative and competitive reduction factors, respectively. In our implementation, the cooperative action corresponds to a 30% reduction ($\gamma_c = 0.30$), while the competitive action corresponds to a 10% reduction ($\gamma_k = 0.10$). These values capture the ability of users to temporarily reduce non-essential consumption in exchange for cost or resilience benefits, [8].

Since both users act simultaneously, the total DR-adjusted demand becomes (21):

$$L_{\mathrm{tot}}(t) = L_1^{\mathrm{DR}}(t) + L_2^{\mathrm{DR}}(t). \tag{21}$$

In this way, we have:

Lemma 1 (Impact of DR Actions on Aggregate Demand)**.** *For two users with baseline demands L_1, L_2, the total demand under strategy*

$a \in \{coop, comp\}$ satisfies (equation 22):

$$L^a_{tot} = (1 - \gamma_a)(L_1 + L_2), \tag{22}$$

where $\gamma_{coop} = 0.3$, $\gamma_{comp} = 0.1$.

4.3 Strategic Interaction Between Users

The decision to cooperate or compete can be interpreted in the context of strategic user behavior. Cooperative actions relieve stress on the microgrid by reducing renewable deficits and limiting battery discharge, thereby contributing to system-level resilience. Competitive actions preserve user comfort and consumption preferences but offer less support to the system.

While users may have inherent preferences for either strategy, their ultimate decision depends on the microgrid's operating conditions, particularly renewable availability and battery state. As described in Section 5, each action leads to different operational outcomes under the renewable scenarios, and the risk-aware optimization framework determines the preferred strategy by minimizing the Uncertainty Cost Function (UCF).

4.4 Impact of Demand Response on Microgrid Operation

The DR-adjusted demand directly influences the energy balance constraint in (18). Cooperative actions mitigate the risk of renewable shortfalls by lowering the effective load, while competitive actions increase the likelihood of discharging the battery or incurring operational costs. In addition, DR affects the evolution of the State of Charge (SOC) through the SOC update equation in (16). These interactions highlight the role of DR as a flexible, user-dependent mechanism for shaping the microgrid's response to uncertainty.

The integration of DR within a risk-aware decision-making process enables the microgrid to leverage user flexibility not only for cost reduction but also for enhancing robustness against extreme renewable events. This connection is formalized in the next section, where we introduce the scenario-based Uncertainty Cost Function and the optimization framework used to select the optimal DR action at each time step, [5], [14].

5 Algorithm Description

This section presents the complete procedure used to compute the optimal demand response (DR) action at each hour under renewable uncertainty. The algorithm integrates scenario generation, operational cost evaluation, risk quantification through CVaR, SOC analysis, and minimization of the Uncertainty Cost Function (UCF). The process is executed independently for each hour of the 24-hour scheduling horizon, enabling the microgrid to react dynamically to changing conditions, [2], [7], [11].

5.1 Inputs and Outputs

The main inputs of the algorithm are:

- Baseline demand profiles $L_1(t)$ and $L_2(t)$ for both flexible users.
- Probabilistic renewable generation models described in Section 2.
- Battery parameters and SOC update model in Section 3.
- DR adjustment factors γ_c and γ_k.
- Number of Monte Carlo scenarios M.
- Weighting coefficients λ_1 and λ_2 in the UCF.
- Time-varying electricity price $c(t)$.

The outputs are:

- The optimal DR action $a^\star(t)$ for each hour.
- The resulting SOC trajectory $SOC(t)$.
- The hour-by-hour uncertainty-aware cost.

5.2 Hourly Optimization Procedure

At each hour t, the microgrid takes the following steps:

1. Generate M independent renewable scenarios using equations (7) and (12).
2. Evaluate the two possible DR actions (cooperative and competitive).
3. For each action:
   (a) Adjust the load.
   (b) Compute the operational cost for each scenario.
   (c) Compute the expected cost.
   (d) Compute VaR and CVaR.
   (e) Estimate the candidate next SOC and compute $\sigma_{\mathrm{SOC}}(t)$.
   (f) Compute the overall UCF.
4. Select the action with minimum UCF.
5. Update the SOC using the chosen action and the SOC dynamics of (16).

5.3 Pseudocode Representation

The complete risk-aware DR optimization procedure is summarized in Algorithm 1 (Table 1.).

Table 1: Algorithm 1. Risk-Aware Demand Response Optimization. Source: created by the authors.

Input: $L_1(t)$, $L_2(t)$, $SOC(0)$, γ_c, γ_k, M, λ_1, λ_2, $c(t)$
for $t = 1$ to 24 **do**
  Generate renewable scenarios $\{P^m_{\text{RES}}(t)\}^M_{m=1}$
  for each action $a \in \{\text{coop}, \text{comp}\}$ **do**
    Compute $L^a_{\text{tot}}(t)$ using equations (20) and (21)
    Evaluate costs $\{C^{m,a}_{\text{op}}(t)\}^M_{m=1}$
    Compute $\mathbb{E}[C^a_{\text{op}}(t)]$
    Compute $\text{VaR}^a_\alpha(t)$ and $\text{CVaR}^a_\alpha(t)$
    Estimate candidate $SOC^a_{\text{cand}}(t)$
    Compute $\sigma^a_{\text{SOC}}(t)$
    Compute $\text{UCF}^a(t)$
  end for
  Select $a^\star(t) = \arg\min_a\{\text{UCF}^a(t)\}$
  Update $SOC(t+1)$ using (16)
end for
Output: $\{a^\star(t)\}$, $\{SOC(t)\}$

The proposed algorithm ensures that DR decisions reflect not only typical operating conditions but also extreme renewable shortfalls, [2]. By evaluating each action over multiple scenarios and minimizing a multi-component risk measure, the microgrid achieves improved resilience, reduced SOC volatility, and increased protection against tail events.

In this way, we have:

Lemma 2 (Algorithm Complexity)**.** *The proposed algorithm has complexity $O(24 \cdot M)$, where M is the number of scenarios.*

Theorem 2 (Monte Carlo Sampling Convergence)**.** *Under the assumptions of independence and correct distribution of scenarios, the estimator of $\mathbb{E}[C_{\text{op}}]$ converges in probability to the true value as $M \to \infty$.*

6 Numerical Results and Discussion

This section presents the numerical evaluation of the proposed risk-aware demand response (DR) strategy using the probabilistic renewable models and the optimization framework described previously. A 24-hour horizon was simulated with $M = 100$ Monte Carlo scenarios per hour, enabling a detailed characterization of uncertainty and its impact on operational decision-making.

6.1 Renewable Uncertainty Characterization

The solar and wind generation scenarios exhibit markedly different statistical behaviors due to the physical and temporal characteristics of each resource. Solar irradiance is strictly limited to daylight hours and follows a smooth bell-shaped profile, whereas wind speed remains highly stochastic throughout the day.

Figure 4 summarizes the solar generation scenarios through hourly boxplots. The distribution presents a clear peak around midday, with reduced dispersion at sunrise and sunset. No production occurs during night hours, which confirms the physical consistency of the model as in [7].

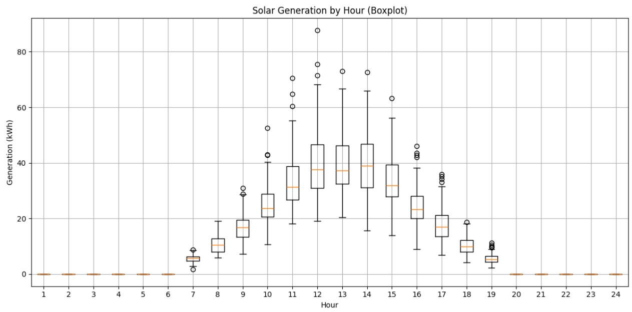

Fig. 4: Solar generation scenarios summarized by hourly boxplots (M = 100). Source: created by the authors.

Wind generation, shown in Figure 5, displays significantly higher variability. The interquartile range remains wide across all hours, and extreme outliers are frequent, reflecting the intermittent and rapidly fluctuating nature of wind resources. This high dispersion directly increases operational uncertainty and magnifies the importance of risk-aware optimization, [12].

6.2 Impact of UCF on Operational Strategy

The proposed Uncertainty Cost Function (UCF) incorporates expected cost, CVaR, and battery SOC stability. Figure 6 shows the optimal DR action selected at each hour. Cooperative behavior dominates during hours of high renewable uncertainty or low battery charge, whereas competitive actions appear only when the system is sufficiently stable.

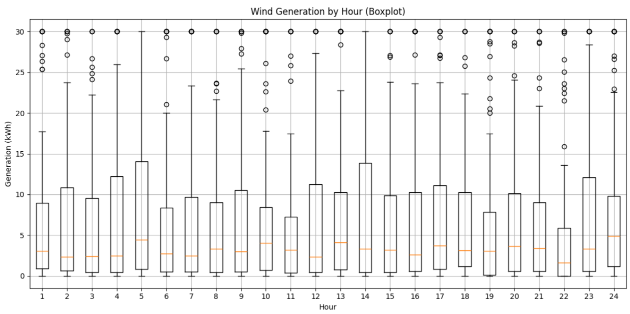

Fig. 5: Wind generation scenarios summarized by hourly boxplots (M = 100). Source: created by the authors.

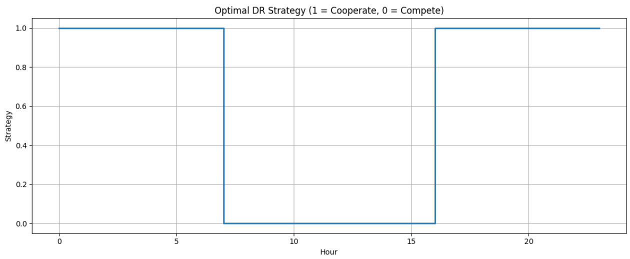

Fig. 6: Optimal DR strategy selected by the UCF (1 = Cooperate, 0 = Compete). Source: created by the authors.

6.3 Effect on Battery State-of-Charge (SOC)

Figure 7 compares the SOC trajectory with and without UCF. The baseline case exhibits large oscillations and several deep discharge events, which pose risks to system reliability. In contrast, the UCF-based strategy maintains a significantly smoother SOC trajectory with fewer extreme deviations. This reflects the contribution of the σ_{SOC} penalty term in avoiding aggressive charge/discharge cycles.

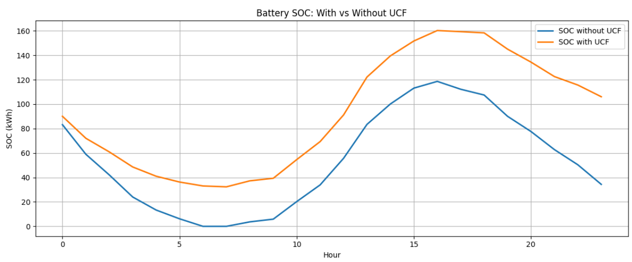

Fig. 7: Battery State-of-Charge (SOC) with and without UCF. Source: created by the authors.

Beyond cost savings, the proposed approach also helps stabilize battery performance by reducing fluctuations in the state of charge. By directly penalizing SOC variability within the UCF, the strategy discourages aggressive charge–discharge cycles, leading to steadier operation and potentially extending the battery's lifetime.

6.4 Cost and Risk Reduction

Hourly operating costs are shown in Figure 8. The UCF formulation systematically reduces high-cost events by mitigating renewable deficits through cooperative DR and more conservative SOC management, [1], [18].

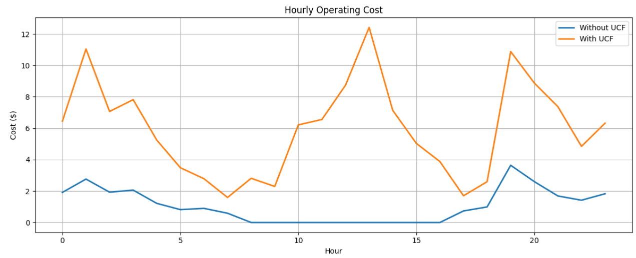

Fig. 8: Hourly operating cost with and without UCF. Source: created by the authors.

This trend becomes more evident when examining cumulative cost (Figure 9). Over the 24-hour horizon, the UCF approach achieves a net cost reduction while also reducing the tail risk, as quantified by CVaR.

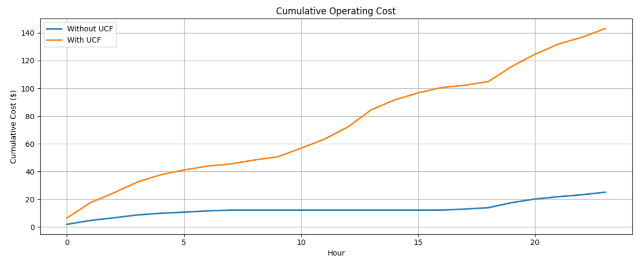

Fig. 9: Cumulative operating cost without UCF vs. with UCF. Source: created by the authors.

These results demonstrate that incorporating CVaR into the decision process effectively reduces exposure to extreme renewable scenarios. By balancing economic performance, risk, and battery stability, the UCF strategy consistently outperforms the deterministic baseline and provides a more robust operational policy for uncertain microgrid environments.

7 Conclusions

This work introduced an uncertainty-aware dispatch framework for renewable-based microgrids, integrating stochastic renewable generation, energy storage behavior, and demand response into a single convex optimization problem through a lightweight Uncertainty Cost Function (UCF).

The simulation results demonstrate that explicitly accounting for risk can substantially reduce extreme operating costs compared to a deterministic baseline, especially during peak demand, while also ensuring more stable battery operation. The proposed framework achieves a balance between modeling accuracy and computational efficiency, making it well suited for real-time microgrid management.

Looking ahead, future research will focus on extending the approach to more advanced demand response schemes and validating its performance in real microgrid environments.

Appendix: Proofs of 2.1 and 5.1

Proof of Theorem 2.1. By the Strong Law of Large Numbers, the sample average converges almost surely to the expected value. The result follows from the continuous mapping theorem.

Proof of Theorem 5.1. The convexity of UCF follows from the convexity of CVaR and the linearity of expectation. The sum of convex functions is convex.

References:

[1] J. Hetzer, D. C. Yu and K. Bhattarai, "An Economic Dispatch Model Incorporating Wind Power," in IEEE Transactions on Energy Conversion, vol. 23, no. 2, pp. 603-611, June 2008, https://doi.org/10.1109/TEC.2007.914171.

[2] T. Clavier, Nima Razavi-Ghods, François Glineur, David González-Ovejero, Eloy de Lera Acedo, Christophe Craeye, "A Global-Local Synthesis Approach for Large Non-Regular Arrays," in IEEE Transactions on Antennas and Propagation, vol. 62, no. 4, pp. 1596-1606, April 2014, https://doi.org/10.1109/TAP.2013.2284816.

[3] J. Zhao, F. Wen, Z. Y. Dong, Y. Xue and K. P. Wong, "Optimal Dispatch of Electric Vehicles and Wind Power Using Enhanced Particle Swarm Optimization," in IEEE Transactions on Industrial Informatics, vol. 8, no. 4, pp. 889-899, Nov. 2012, https://doi.org/10.1109/TII.2012.2205398.

[4] S. Surender Reddy, P. R. Bijwe and A. R. Abhyankar, "Real-Time Economic Dispatch Considering Renewable Power Generation Variability and Uncertainty Over Scheduling Period," in IEEE Systems Journal, vol. 9, no. 4, pp. 1440-1451, Dec. 2015, https://doi.org/10.1109/JSYST.2014.2325967.

[5] Cardell, J. B., Anderson, C. L.: Analysis of the system costs of wind variability through Monte Carlo simulation. Presented at the 43rd Hawaii International Conference on System Sciences (HICSS), Honolulu, HI, 2010, pp. 1–8, https://doi.org/10.1109/HICSS.2010.61.

[6] Anderson, C. L., Cardell, J. B.: Analysis of wind penetration and network reliability through Monte Carlo simulation. Presented at the 2009 Winter Simulation Conference (WSC), Austin, TX, 2009, pp. 1503–1510, https://doi.org/10.1109/WSC.2009.5429298.

[7] Thomopoulos, N.: Essentials of Monte Carlo simulations. Statistical methods for building simulation models, Illinois Institute of Technology, ISBN 978-1-4614-6021-3, Springer Science (2013), https://doi.org/10.1007/978-1-4614-6022-0.

[8] Tomás Valencia-Zuluaga, Daniel Agudelo-Martinez, Dario Arango-Angarita, Camilo Acosta-Urrego, Sergio Rivera, Diego Rodríguez-Medina, "A Fast Decomposition Method to Solve a Security-Constrained Optimal Power Flow (SCOPF) Problem Through Constraint Handling," in IEEE Access, vol. 9, pp. 52812-52824, 2021, https://doi.org/10.1109/ACCESS.2021.3067206.

[9] Meng, J., Li, G., Du., Y.: Economic dispatch for power systems with wind and solar energy integration considering reserve risk. Presented at Power and Energy Engineering Conference (APPEEC), 8-11 Dec., 2013, https://doi.org/10.1109/APPEEC.2013.6837207.

[10] Guo, Q., Han, J., Yoon, M., Jang, G.: A study of economic dispatch with emission constraint in smart grid including wind turbines and electric vehicles. Presented at the Vehicle Power and Propulsion Conference (VPPC), 9-12 Oct., 2012, pp. 1002–1005, https://doi.org/10.1109/VPPC.2012.6422753.

[11] Xie, F., Huang, M., Zhang, W., Li, J.: Research on electric vehicle charging station load forecasting. Presented at International Conference on the Advanced Power System Automation and Protection (APAP), 2011, https://doi.org/10.1109/APAP.2011.6180772.

[12] Sufen, T., Youbing, Z., Jun, Q.: Impact of electric vehicles as interruptible load on economic dispatch incorporating wind power. Presented at the International Conference on Sustainable Power Generation and Supply (SUPERGEN 2012), 8-9 Sept., 2012, https://doi.org/10.1049/cp.2012.1816.

[13] D. Midence, S. Rivera and A. Vargas, "Reliability assessment in power distribution networks by logical and matrix operations," 2008 IEEE/PES Transmission and Distribution Conference and Exposition: Latin America, Bogota, Colombia, 2008, pp. 1-6, https://doi.org/10.1109/TDC-LA.2008.4641696.

[14] S. Mohseni and A. C. Brent, "A non-cooperative game-theoretic approach for the flexible operation of multi-microgrids," 2023 IEEE Power Energy Society General Meeting (PESGM), Orlando, FL, USA, 2023, pp. 1-5, https://doi.org/10.1109/PESGM52003.2023.10253073.

[15] Mahdi Azimian, Reza Habibifar, Vahid Amir, Elham Shirazi, Mohammad Sadegh Javadi, Ali Esmaeel Nezhad, "Planning and Financing Strategy for Clustered Multi-Carrier Microgrids," in IEEE Access, vol. 11, pp. 72050-72069, 2023, https://doi.org/10.1109/ACCESS.2023.3294482.

[16] S. Mohseni and A. C. Brent, "Maximizing the Utilization of Demand Response in Multi-Microgrids: A Game-Theoretic Approach," 2024 IEEE Power Energy Society General Meeting (PESGM), Seattle, WA, USA, 2024, pp. 1-5, https://doi.org/10.1109/PESGM51994.2024.10688921.

[17] Y. Yao, Y. Xu, W. Gu, K. Liu, S. Lu and L. Mili, "Inverse Uncertainty Quantification Assisted Forward Uncertainty Quantification in Power System Dynamic Simulations," in IEEE Transactions on Power Systems, vol. 40, no. 5, pp. 4307-4321, Sept. 2025, https://doi.org/10.1109/TPWRS.2025.3537758.

[18] A. Latifi and C. M. Scoglio, "A Survey on Uncertainty Quantification in Dynamical Systems," in IEEE Transactions on Systems, Man, and Cybernetics: Systems, vol. 55, no. 8, pp. 5137-5151, Aug. 2025, https://doi.org/10.1109/TSMC.2025.3564984.

Contribution of Individual Authors to the Creation of a Scientific Article (Ghostwriting Policy)

The authors equally contributed in the present research, at all stages from the formulation of the problem to the final findings and solution.

Sources of Funding for Research Presented in a Scientific Article or Scientific Article Itself

No funding was received for conducting this study.

Conflict of Interest

The authors have no conflicts of interest to declare that are relevant to the content of this article.